



Synthesis 4-(4'-methylphenyl)-2-mercaptothiazole Structure with NMR, Vibrational, Mass Spectroscopy and DFT Studies

REZA SOLEYMANI^{1*}, REIHANEH DEGHANIAN DIJVEJIN²,
ASIYE FALLAHI GOZAL ABAD HESAR² and EBTESAM SOBHANIE²

¹Young Researchers Club, Shahre-rey Branch, Islamic Azad University, Tehran, Iran.

²Department of Chemistry, Shahre-rey Branch, Islamic Azad University, Tehran, Iran.

*Corresponding author: E-mail address: reza.soleymani@hotmail.com

(Received: May 27, 2012; Accepted: June 30, 2012)

ABSTRACT

4-(4'-methylphenyl)-2-mercaptothiazole (MPMT) was synthesized from a compound of thiocarbamate family using condensation reaction. The spectroscopic properties of this structure were studied using ¹H-NMR, ¹³C-NMR, FT-IR, Mass Spectroscopy, and elemental analysis methods. Subsequently, its thermodynamic parameters were examined by performing density functional theory (DFT) calculation at B3LYP, B3PW91, and mPW1PW91 levels of theory and 6-311G (d, p) basis set. After studying the values of total energy, entropy, vibrational frequencies, ZPVE, HOMO and LUMO dependant parameters such as Chemical potential, Chemical hardness, Electrophilicity, and maximum amount of electronic charge transfer were also considered. However, chemical shift value of different nuclei were theoretically determined. The results indicated high conformity between the theoretical and experimental values. Finally, the electrostatic potential values of this structure were studied. The results showed variation in the value of this parameter at different part of the structure.

Key words: FT-IR, Mass Spectroscopy, mPW1PW91, NMR, Synthesis.

INTRODUCTION

Thiazoles are five-membered heterocyclic compounds, containing carbon, sulfur, and nitrogen atoms in the ring. Due to their myriad biological activities, these compounds are used in various industries such as pharmaceutical, paint, and complex chemicals. The first of these compounds was initially identified by Hantzsch *et al.*, and his colleague, Weber *et al.*, on 18 November 1887. The first derivative of Thiazole was produced by J. Popp *et al.*, in 1889¹⁻¹⁷. This compound exists

in the chemical structure of vitamin B1. The vitamin, also known as thiamine, is water soluble and is composed of a Thiazole and a Pyrimidine heterocyclic ring. Its Thiazole ring has the structure of 4-methyl-5-(hydroxyethyl)thiazole. The rings are linked through the N of the Thiazole ring and C₅ of the Pyrimidine ring. Due to containing sulfur and nitrogen groups, these compounds show a high tendency to participate in various chemical reactions, including alkaalisation, oxidation and cycloadditions¹⁶⁻¹⁷. Thiazoles are also used as antihyperglycemic compounds⁷. They have also

displayed anti-tumor, antibacterial, anti-viral, anti-malaria and anthelmintic activities¹⁸. Because of their antifungal properties, many Thiazoles derivatives have also been synthesized for pharmaceutical purposes¹⁻¹². These compounds are also used in agriculture for the production of insecticides and pesticides⁸⁻¹⁵. Furthermore, these compounds are also used in the synthesis of re-shift catalysts. The synthesis of these compounds is possible through various catalysts which affect the reaction rate. The spectacular properties of these compounds induced us to study the synthesis, identification, and some thermodynamic parameters of one of their derivatives. HOMO and LUMO dependant parameters such as chemical potential, chemical hardness, Electrophilicity, and maximum amount of electronic charge transfer are also considered. Electrophilicity is a HOMO and LUMO dependant parameter which affects the reactivity of the structure¹⁹. In fact, Electrophilicity is proportional to ionization potential and electronic effects. This parameter is calculated by equation (1). The parameters of chemical potential and chemical hardness can also be calculated by equations (2) and (3). These parameters are correlated to HOMO and LUMO values; thus, their values are different for various compounds. In fact, it is expected that chemical potential changes as electronegative value changes. As electronic potential increases, chemical hardness decreases and we will have a good electrophone species. The maximum transferred electronic charge can be calculated by equation (4)^{19, 20, 21}. In reactions such as Friedel-Crafts reactions, Electrophilicity correlates with the yield of the reaction. It is also believed that in some reactions Electrophilicity correlates with the stability of the structure²².

$$\Omega = \mu^2 / 2\eta = \chi^2 / 2\eta \quad \dots(1)$$

$$\chi = -\mu = -(\delta_E / \delta_{N_{VI}}) \approx (I+A) / 2 \approx -1/2 (\epsilon_{HOMO} + \epsilon_{LUMO}) \quad \dots(2)$$

$$\eta = (\delta_{2E} / \delta_{N_{VI}}) = (I-A) \approx (\epsilon_{LUMO} - \epsilon_{HOMO}) \quad \dots(3)$$

$$\Delta N_{max} = -\mu / \eta \quad \dots(4)$$

EXPERIMENTAL

General method

All of chemical materials were purchased from Germany firm Merk. For this study, all of instruments that were used, are as follows: microwave oven model LG-SOLARDOM LF-

5901WCR, Japanese weighing with 0.100 g sensivity model ANDGF-300, hitter and stirrer model Heidolphm Rn3004 Safty, Merk thin layer chromatography sheets Art no: 1:0554, Electrothermal melting point measurement apparatus, Memmert (oven) materials and glossy instruments desiccators (oven), vacuum pump Emerson model: C55-JJXH4205, Rmp: 1425/1725, Heidolph model: Labrota rotary solution. ¹H-NMR and ¹³C-NMR spectra studying done by Bruker Avance 300 spectrometer with the processing software XWINNMR version 3.1. measured. Chemical shifts of TMS. FT-IR by a Perkin Elmer spectrum 1420 spectrometer in the frequency range of 4000–400cm⁻¹ using KBr discs are reported on 1 scale. The FT-IR spectra were recorded at room temperature at the spectral resolution of 1 cm⁻¹. Used Glossy instruments are as follows: one and two ports round- bottom emery-top flasks species, simple, bubble and spiral radiator, Erlenmeyer flask, beakers, three and two ports, links, addition funnel, Buchner funnel, capillary tube and etc.

Synthesis

12.50 g (0.04 mol) 4-bromo phenacyl bromide was solved in 212.5 mL ethanol and 9.3 g (0.08 mol) ammonium di-thio carbamate was added to it and was refluxed for 3 hours. After ejecting of solvent by rotary, the yellow solid was formed that was refluxed for 15 minutes by 125.0 mL benzene. Than obtained solution was become cold and crystal precipitation was formed. Finally, the precipitation was strained and dried. 18.0 g production, 86% yield and 191-193 °C melting point was produced. TLC chromatogram and comparison of its R_f by 4-methyl phenacyl bromide R_f was established forming of production and its purity. The residue was purified by thin layer chromatography on silica gel (85:15 cyclo hexane-acetone) to give (18 g, 86%);

A yellow solid; Mp: 191-193; IR (KBr): 3153, 3081, 3018, 2932, 2595, 1597, 1433, 1243, 1098, 814, 694, 512. ¹H-NMR (400 MHz, CDCl₃) δ: 2.50 (s, 3H, CH₃), 3.16 (s, 1H, SH Aliphatic), 6.92 (s, 1H, H-5), 7.28-7.30 (J=9Hz, d, 2H, 3-H',5-H'), 7.48-7.49 (d, 2H, 2'-H,6'-H). ¹³C-NMR (CDCl₃) δ: 23.12, 118.01, 128.93, 132.33, 132.92, 133.12, 134.38, 145.01, 158.99, 169.63. Anal. Calcd for C₁₀H₉NS₂: C, 57.93; H, 4.38; N, 6.76; S, 30.93, Found: C, 56.85; H, 3.16; N, 6.55; S, 30.78. *m/z*: 207.16 (100.0%), 208.12

(12.5%), 209.33 (9.0%).

Computational details

All calculations were made on a personal computer (Intel Core i7 CPU 1.7 GHz and 4.00 GB of RAM) with Microsoft Windows XP® system. The experiment was carried out under gas state at 1 atmospheric pressure and a temperature of 298 K. Firstly; the structure under study was pre-designed by Gauss View software²³ and then its energy was pre-optimized using AM1 semi-experimental method. Subsequently, the values of thermodynamic parameters, vibrational frequencies, and chemical shifts were calculated using the Gaussian 03W software package²⁴. DFT calculation was performed at 6-311G (d, p) basis set²⁵⁻²⁹. In order to approximate the obtained results to the experimental values, 0.967, 0.963 and 0.957 scaled factors were applied for three levels of B3LYP, B3PW91, and mPW1PW91, respectively. The electrostatic potential values were also examined for this structure using Molekel 5.4 software. The results of vibrational frequencies were analyzed using VEDA 4 software³⁰. The values of NMR parameters were calculated by GIAO method³¹. All results were reported by taking Tetra Methyl Silane (TMS) as reference. Finally, Chemical potential, Chemical hardness, Electrophilicity, and maximum amount of electronic charge transfer were studied using HOMO and LUMO dependant parameters.

RESULTS AND DISCUSSION

MPMT structure was experimentally synthesized in laboratory (Fig. 1) and the values of the vibrational frequencies, chemical shifts, electrostatic potential of the different parts of the structure, and HOMO and LUMO dependant parameters were calculated. The results are interpreted below (Fig. 1 and 2).

Vibrational assignments

After the optimization of the structure by DFT calculation method, the values of vibrational frequencies were analyzed using VEDA 4 software. MPMT structure consists of 19 atoms and has 60 normal vibrational mod nos. The theoretically obtained results were compared with the experimental results. As it was mentioned, the scaled factors of 0.967, 0.963 and 0.957 were

respectively applied for the three theoretical levels of B3LYP, B3PW91, and mPW1PW91 to increase the conformity between theoretical and experimental results (Fig. 3).

C-H vibrations

The type of C-H vibration varies depending on the bond hybridization and level. The sp^2 hybridized C-H bonds usually give a visible band above 3000 cm^{-1} (i.e. $3000\text{-}3100\text{ cm}^{-1}$) while the sp^3 hybridized C-H bonds give a visible band below 3000 cm^{-1} (i.e. $2800\text{-}3000\text{ cm}^{-1}$)³²⁻³⁴. There are different types of C-H bond in the structure of MPMT showing different vibrational frequencies. According to the experimental results, C-H stretching vibration was visible in the region $2932\text{-}3153\text{ cm}^{-1}$. This showed a good agreement with the theoretical results. The frequency of the C-H stretching vibration was observed in $2922\text{-}3154$, $2902\text{-}3130$, and $2918\text{-}3147\text{ cm}^{-1}$ using B3LYP, B3PW91, and mPW1PW91 methods, respectively. PEDs analysis also confirms the obtained results (Table 1). The stretching vibrations appeared in in-plane and out-of-plane forms and gave moderate to strong peaks. C-H bending vibration was also observed in different regions. This vibration is visible in the region $1100\text{-}1480\text{ cm}^{-1}$. The experimental results showed that, in MPMT structure, this vibration can be clearly observed at the frequency of 1433 cm^{-1} . The theoretical methods also showed the C-H bending vibration in different regions and confirmed the experimental results.

C-S vibrations

Many resources has reported that the C-S stretching vibration in BPMT structure is visible in region $600\text{-}750\text{ cm}^{-1}$ ³⁵, however, there are some resources which has reported that it is visible in $680\text{-}710\text{ cm}^{-1}$ or $609\text{-}716\text{ cm}^{-1}$ ³⁶⁻³⁷. The stretching vibration in MPMT was observed in 746 cm^{-1} using experimental method and below 1022 cm^{-1} using B3LYP, B3PW91, and mPW1PW91 methods. Therefore, this vibration occurred in different regions. PEDs analysis confirmed the obtained results.

C-N and C=N vibrations

C-N stretching vibration also varies in different structures. Generally, we expect to observe this vibration in region $1000\text{-}1250\text{ cm}^{-1}$. However,

Table 1: Vibrational wavenumbers obtained for MPMT structure at B3LYP, B3PW91 and mPW1PW91 method [harmonic frequency (cm⁻¹), IRint (Kmmol⁻¹)].

Mod nos	Experimental (cm ⁻¹)	Theoretical wave number (cm ⁻¹)					
		B3LYP		B3PW91		mPW1PW91PED(%) ^c	
	FT-IR	Scaled	IR _{int} ^b	Scaled	IR _{int} ^b	Scaled	IR _{int} ^b
1		9	0.0311	8	0.0543	9	0.015
2		24	0.1759	24	0.2056	23	0.2775
3		63	0.6689	62	0.857	63	0.8856
4		96	0.0413	94	0.0376	94	0.0317
5		153	10.2967	157	1.1544	158	0.7039
6		165	11.5038	172	19.6886	175	20.1583
7		213	5.1875	213	6.2801	215	6.0937
8		218	2.4149	216	3.7347	218	4.418
9		278	1.9704	276	1.8829	278.	1.8624
10		315	1.161	312	1.0035	314	1.0307
11		320	1.1601	317	1.482	319	1.5355
12		381	0.6166	380	0.7519	383	0.6838
13		401	0.1025	394	0.1149	396	0.0966
14		477	7.6088	472	9.1959	476	9.6471
15		486	2.4512	482	2.2764	486	2.246
16	512vw	519	1.1086	515	1.0875	520	0.9349
17		559	5.1152	555	4.8338	559	4.8051
18		618	11.2157	621	5.8478	626	1.8291
19		634	0.1921	626	4.1667	633	7.3948
20		661	0.0433	655	0.0534	660	0.0352
21	694m	683	25.9025	674	28.547	680	26.9211
22		727	30.442	718	30.3387	723	32.3025
23		766	10.0503	765	6.818	770	6.2777
24		806	16.0814	799	19.2106	805	19.5156
25		809	10.9408	815	11.6195	823	11.5981
26	814w	829	9.4152	819	8.8713	826	8.249
27		872	37.7066	867	42.7444	874	42.4197
28		882	11.5019	876	2.6433	882	2.4003

29		929	0.2351	921	0.3998	928	0.4847	38vSCN+35THCCC+16TCCCC
30		958	0.7961	948	0.8332	956	0.9066	19THCCC+45THCCC+28TCCCC
31		971	4.4504	957	4.6961	963	3.4076	10vCC+12δHCH+23THCCC+32HCCC
32		1001	4.3739	989	4.0975	995	3.4995	39δCCC+22δCCC+15δCCC
33		1022	72.0411	1009	8.0467	1015	10.2225	19vSC+15δHSC+32δCNC
34		1026	6.5694	1026	70.6972	1037	49.9415	12δHCH+49THCCC+11TCCCC
35		1044	28.1153	1038	31.6375	1046	52.2386	22vNC+31δHCS
36	1098vw	1104	10.1284	1091	13.1021	1096	14.0894	10vCC+12vCC+17δHCC+17δHCC+15δHCC+10δHCC
37		1170	7.9537	1153	7.587	1159	7.63	24δHCC+16δHCC+13δHCC+15δHCC
38		1179	2.0008	1172	2.7129	1181	2.7449	19vCC+10vCC+10vCC+10δHCS
39		1198	2.1932	1189	0.998	1198	0.6851	27vCC+11vHCC+11vHCS
40	1243w	1256	24.4269	1257	17.0913	1266	14.2413	12vCC+22vCC+21vNC+10vCC
41		1288	11.9644	1284	6.4927	1291	4.8289	10vCC+13vCC+18vCC+10vCC
42		1302	15.448	1301	28.5393	1311	35.3042	22δHCC+15δHCC+11δHCC+17δHCC
43		1367	0.0124	1344	0.2361	1352	0.248	30δHCH+22δHCH+42δHCH
44		1393	6.3986	1381	5.1364	1390	5.546	20vCC+16vCC+11δHCC+10δHCC
45		1439	7.4876	1416	7.7349	1424	7.859	36δHCH+44δHCH+12THCCC
46	1433m	1442	50.438	1424	15.7913	1431	15.9173	65vNC+10vCC
47		1445	15.487	1438	35.828	1451	29.7299	15δHCH+16δHCH+37δHCH
48		1476	114.56	1468	135.18	1482	144.46	24vNC+30vCC
49		1511	7.5815	1504	3.9672	1519	2.0225	18vCC+16vCC+10δHCC+138HCC
50		1557	0.4939	1554	0.4031	1568	0.5684	23vCC+23vCC+11δCCC
51	1597m	1601	1.2244	1598	1.4448	1613	1.6474	29vCC+13vCC
52	2595w	2587	0.9095	2584	1.9628	2604	2.43	100vSH
53	2932m	2922	39.2793	2902	36.4126	2918	35.1736	17vCH+29vCH+54vCH
54		2970	20.909	2959	17.2161	2978	17.4035	54vCH+42vCH
55		3000	17.8174	2988	15.3142	3006	14.7928	79vCH+17vCH
56	3018vs	3050	16.542	3030	14.6251	3048	14.4257	83vCH+16vCH
57		3055	23.5473	3035	20.4625	3053	19.8098	96vCH
58	3081m	3073	14.3296	3052	12.9518	3070	12.7246	17vCH+82vCH
59		3101	2.19	3076	1.9332	3093	1.8382	97vCH
60	3153s	3154	3.489	3130	3.6874	3147	3.9367	99vCH

^a w-weak; vw-very weak; s-strong; vs-very strong; m-medium; br-broad; sh-shoulder.

^b IR_{int}-IR intensity.

^c Potential energy distribution (PED) calculated B3LYP/6-311G(d,p). v stretching, δ: bending, γ: torsion, λ: out, PED less than 10% are not shown.

in aromatic amines, this variation is observed in region 1200-1330 cm^{-1} . For example, this vibration is observed in 1315 cm^{-1} (FT-IR), 1315 cm^{-1} (FT-Raman), and 1332 cm^{-1} (HF) in Benzoxazole ³⁸. In the structure of MPMT, this vibration was observed in region 1243 cm^{-1} using experimental method and in region 1000-1300 cm^{-1} in B3LYP, B3PW91, and mPW1PW91 using theoretical methods. However,

its C=N stretching vibration was observed in region 1433 cm^{-1} using experimental method and in region 1300-1490 cm^{-1} using theoretical methods. PEDs analysis also confirmed the obtained results.

S-H vibrations

S-H stretching vibration in Thiols is expected to be visible in region 2550-2700 cm^{-1} .

Table 2: Theoretical and experimental ^1H and ^{13}C isotropic chemical shifts (with respect to TMS, all values in ppm) for MPMT structure.

Chemical Shift	Atomic number	Methods			
		B3LYP	B3PW91	mPW1PW91	Exp
	H16	8.35	8.37	8.52	7.49
	H17	7.69	7.68	7.82	7.48
	H14	7.36	7.33	7.45	7.30
	H15	7.33	7.31	7.44	7.28
	H21	7.14	7.09	7.20	6.92
	H22	5.30	5.29	5.42	3.16
	H20	2.57	2.49	2.60	2.50
	H19	2.44	2.36	2.42	2.50
	H18	2.00	1.94	2.08	2.50
	C11	170.70	166.33	166.98	169.63
	C7	159.06	156.65	157.09	158.99
	C2	145.13	142.59	143.22	145.01
	C5	136.93	134.35	134.84	134.38
	C3	134.98	133.61	134.21	133.12
	C1	134.30	132.82	133.46	132.92
	C4	133.76	132.24	132.96	132.33
	C6	129.09	127.68	128.45	128.93
	C9	119.74	117.15	117.14	118.01
	C8	23.74	23.07	23.61	23.12

Table 3. Correlation between theoretical and experimental methods for FT-IR and NMR property in MPMT structure.

Correlation between		Kind of NMR	Equation	R ²
Experimental	B3LYP	^{13}C -NMR	$y = 1.000x + 1.021$	0.999
		^1H -NMR	$y = 0.998x + 0.353$	0.991
		FT-IR	$y = 0.998x + 6.885$	0.999
	B3PW91	^{13}C -NMR	$y = 0.983x + 1.174$	0.999
		^1H -NMR	$y = 1.008x + 0.267$	0.909
		FT-IR	$y = 0.993x + 4.565$	0.999
	mPW1PW91	^{13}C -NMR	$y = 0.983x + 1.627$	0.999
		^1H -NMR	$y = 1.012x + 0.364$	0.908
		FT-IR	$y = 0.998x + 6.815$	0.999

Correspondingly, in the structure of MPMT, this vibration was observed in region 2595 cm^{-1} using experimental method and in 2587 , 2584 , and 2604 cm^{-1} using B3LYP, B3PW91, and mPW1PW91 methods, respectively. However, these vibrations are of moderate to weak intensity. PEDs analysis also confirmed the obtained results. As it is shown in table 1 (mode noise 52), the range of this vibration has appeared 100%.

C-C and C=C vibrations

The type of C=C vibration depends on the position of the bond in the structure. For example, the range of in-ring C=C vibration is expected to be in region $1450\text{-}1650\text{ cm}^{-1}$ while the range of chain C=C vibration is expected to be in region $1850\text{-}2050\text{ cm}^{-1}$, depending on symmetry. In general, according to the wave number ranges given by Varsanyi³⁹ for the five bands in the region, the bands are of variable intensity and are observed in $1625\text{-}1590$, $1590\text{-}1575$, $1540\text{-}1470$, $1465\text{-}1430$, and $1380\text{-}1280\text{ cm}^{-1}$. C-C-C vibrations in DMFP

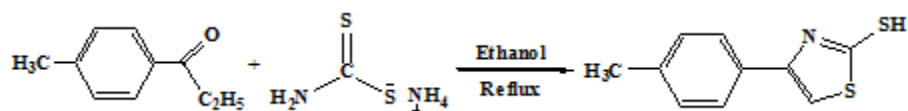
structure showed visible bands at 800 , 618 , 573 , and 483 cm^{-1} of which were similar or very close to the band of this vibration in MPMT structure. In Benzamide oxim, this vibration is observed at 600 and 625 cm^{-1} using experimental method⁴⁰⁻⁴². However, C=C vibration in MPMT has two different forms. It can be in a five- or six-membered ring. In both forms C=C bonds are inside the rings and C-C bonds are between the rings. Depending on the form of C=C bonds inside the rings, the range of chain C=C vibration varies from 1100 to 1650 cm^{-1} . However, the range of C-C-C bending vibration varies from 1100 to 1480 cm^{-1} . The results are displayed in Table 1.

NMR spectra

After the synthesis of MPMT, NMR spectroscopic technique was employed to identify the structure (Fig. 4). TMS was used as the reference substance. In order to verify the experimental results, the chemical shift of different nuclei was also studied by theoretical methods. The

Table 4. Theoretically computed energies (kcal.mol^{-1}), zero-point vibrational energies (kcal.mol^{-1}), rotational constants (GHz), heat capacities ($\text{cal.mol}^{-1}.\text{K}^{-1}$), entropies ($\text{cal.mol}^{-1}.\text{K}^{-1}$), dipole moment (Debye), molecular orbitals energies (ϵ_{HOMO} and ϵ_{LUMO} , eV), electronic chemical potential, μ (eV), chemical hardness, η (eV), electrophilicity, ω (eV) and maximum amount of electronic charge transfer for MPMT structure.

Parameters	B3LYP	B3PW91	mPW1PW91
Total energy	-776600.600	-776427.730	-776535.155
ZPVE	101.387	101.778	102.487
Rotational constant	1.803	1.819	1.825
	0.277	0.278	0.279
	0.240	0.242	0.243
Entropy			
Total	116.740	116.733	116.364
Translational	41.887	41.887	41.887
Rotational	32.256	32.236	32.226
Vibrational	42.597	42.610	42.252
Heat capacity	45.829	45.703	45.404
Dipole moment(D)	1.273	1.261	1.286
HOMO	-0.216	-0.218	-0.224
LUMO	-0.046	-0.047	-0.040
Chemical potential(μ)	-0.131	-0.133	-0.132
Chemical hardness(η)	0.169	0.171	0.184
Electrophilicity(ω)	0.051	0.051	0.047
ΔN_{max}	0.776	0.779	0.721



Scheme 1: Synthetic route for the new compound (MPMT).

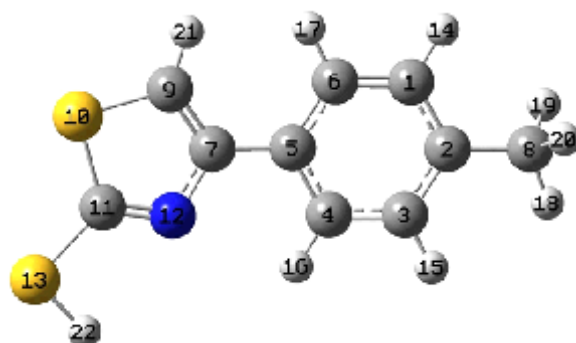


Fig 1. Serial number of atom and optimized structure of MPMT structure performed by B3LYP/6-311G(d,p) method.

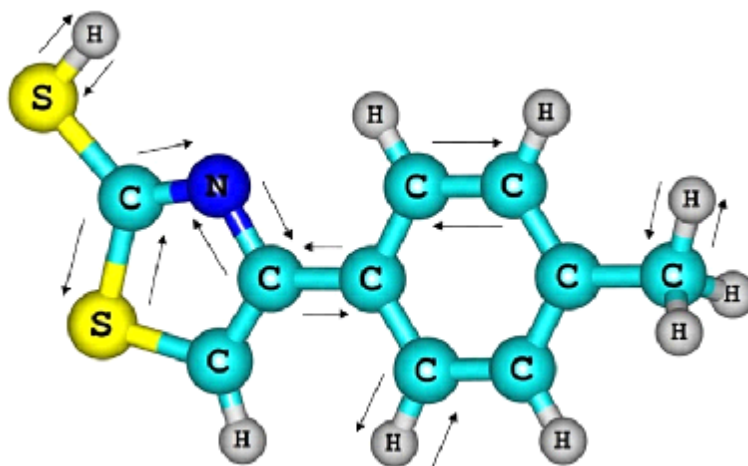


Fig. 2: Show frequency animation in different bond in MPMT structure.

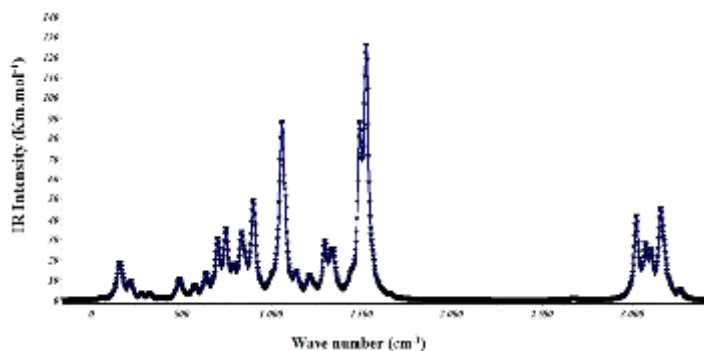


Fig. 3: FT-IR spectrum obtained by B3LYP/6-311G(d,p) method for MPMT structure.

parameters were examined by performing GIAO and DFT calculations at B3LYP, B3PW91, and mPW1PW91 levels of theory and 6-311G (d, p) basis set. The results are reported in Table 2. A good conformity between experimental and theoretical results was observed. As it is displayed in Table 3, the conformity between the results obtained by C-

NMR is better than that obtained by ^1H -NMR. This can be attributed to the fact that the sample is affected by the solvent in ^1H -NMR, while ^{13}C -NMR technique is not dependant on use of a solvent and, therefore, shows a better agreement with the experimental method conducted under gas condition.

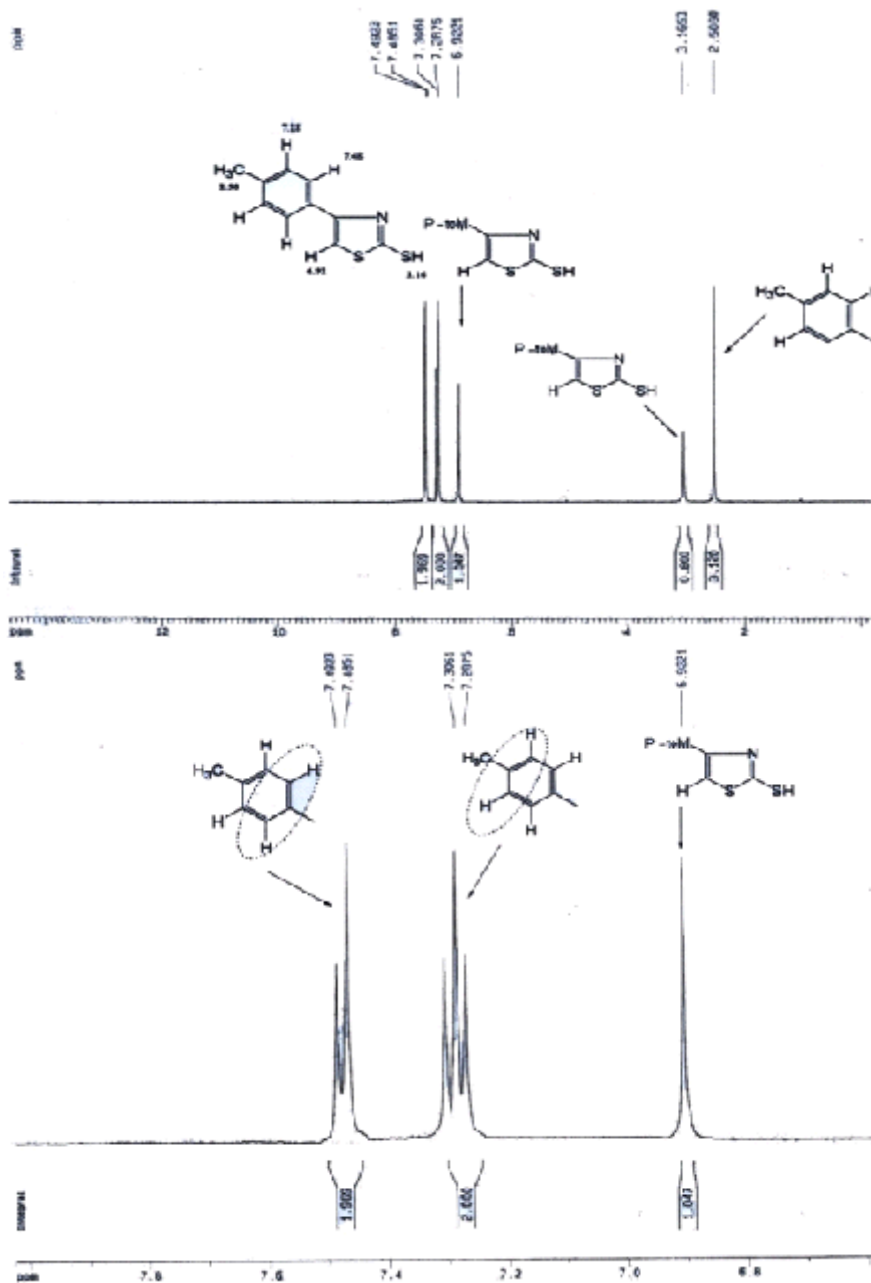


Fig 4. ^1H -NMR spectrum obtained by experimental method for MPMT structure.

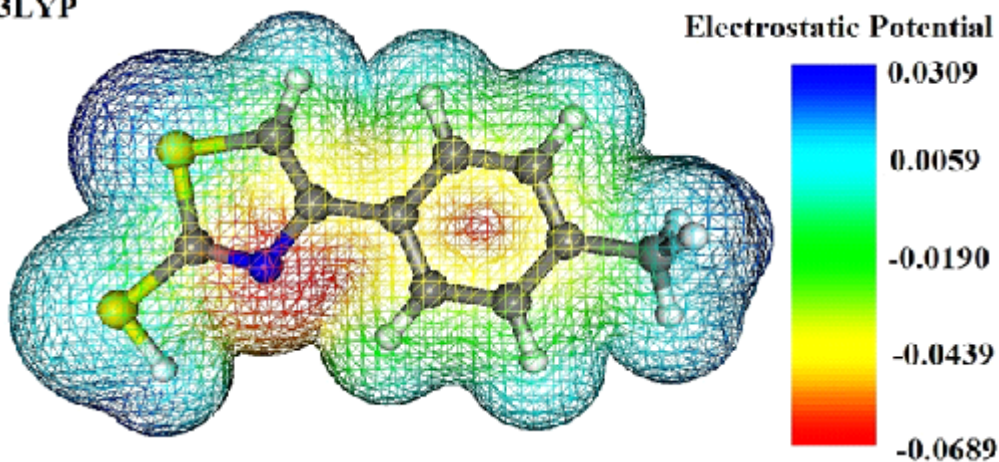
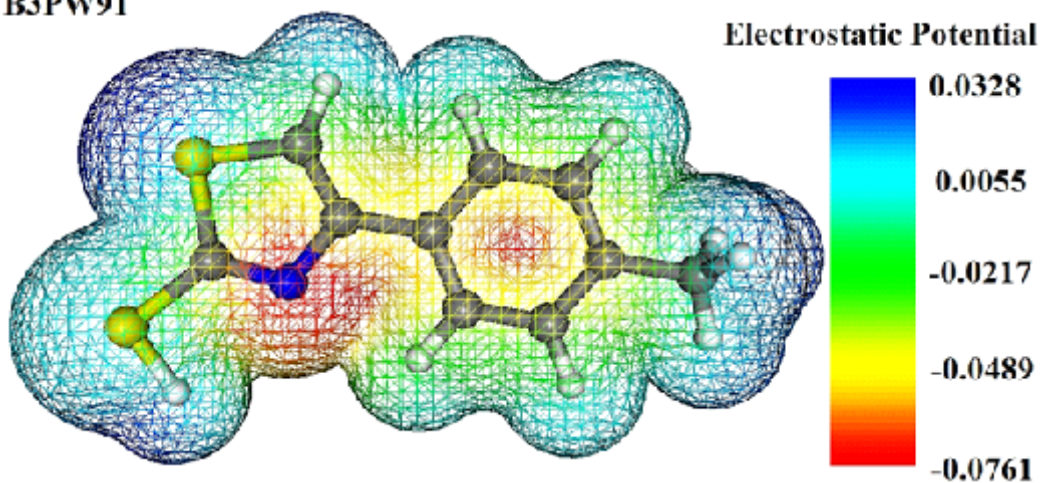
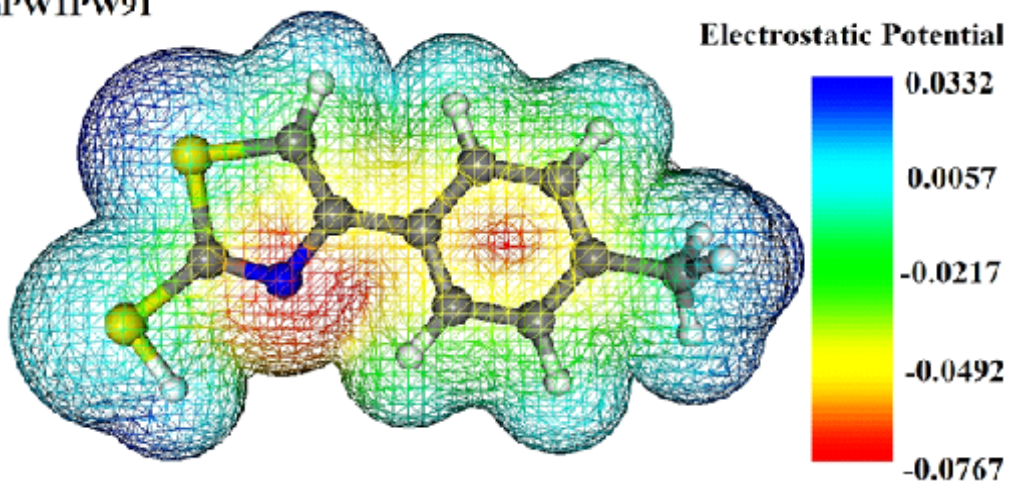
B3LYP**B3PW91****mPW1PW91**

Fig. 5: (a) B3LYP (b) B3PW91 and (c) mPW1PW91 calculated 3D molecular electrostatic potential of MPMT structure (isosurface value 0.01 a.u.).

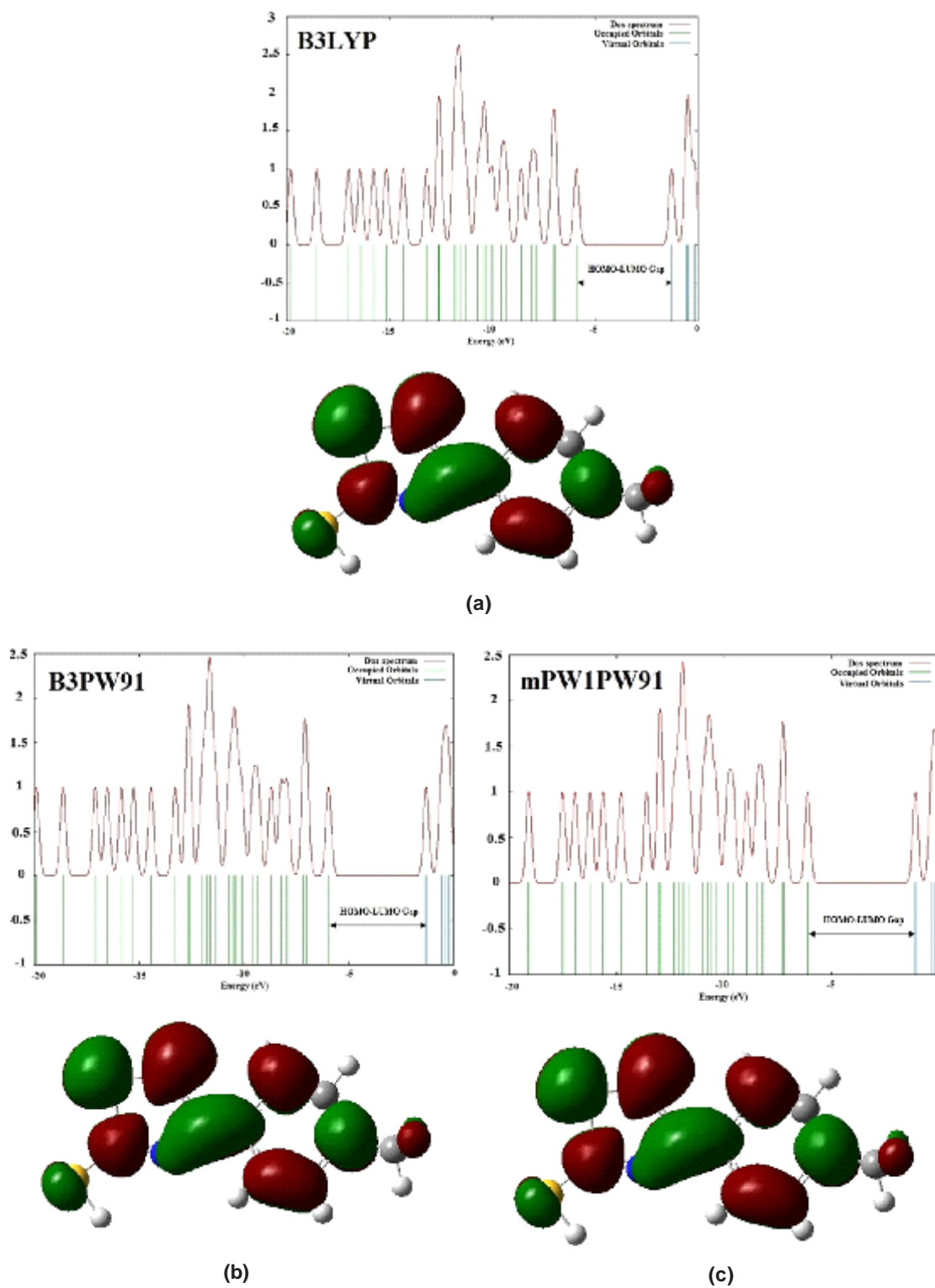


Fig. 6: Partial DOS diagram containing HOMO (left) and LUMO (right) plot of MPMT at (a) B3LYP (b) B3PW91 and (c) mPW1PW91 methods.

Molecular electronic potential maps

Molecular electrostatic potential map (MEPM) illustrates information about electrostatic potential of different parts of a particular chemical structure. MEPM is commonly related to the reactivity of a structure in nucleophilic or electrophilic reactions. It was illustrated for MPMT using DFT calculations at B3LYP, B3PW91, and mPW1PW91 levels of theory and 6-311G (d, p) basis set (Fig. 5). For example, the sections containing nitrogen may be more subjected to the nucleophilic attack because of containing a pair of non bonding electrons. In fact, this map shows reactivity; the more negative is the value for this parameter in a section the more probable is the nucleophilic attack to that sections. As the figure shows, blue sections are less affected by nucleophilic attack and red sections are more affected by nucleophilic attack ⁴³.

HOMO and LUMO indices

Some resources has related HOMO-LUMO gap to the stability of a structure. However, what is evident is that HOMO and LUMO values are completely dependent to the chemical structure of a compound. HOMO and LUMO values were measured for MPMT conducting DFT calculations. Then, HOMO-LUMO gap, Chemical potential, Chemical hardness, Electrophilicity, and maximum amount of electronic charge transferred were considered. The results indicated that HOMO-LUMO gap in MPMT took different values by B3LYP, B3PW91, and mPW1PW91 methods (Fig. 6) (Table 4).

Other molecular properties

Finally, entropy, dipole moment, energy levels, and some other thermodynamic parameters

were studied (Table 4). The experimental results were very close to the theoretical results. We hope the results of this discussion will be helpful in exploring such compounds further.

CONCLUSIONS

This study was conducted to delve into the structure of MPMT using experimental and theoretical methods. As expected, useful results were obtained. After the synthesis of MPMT through the above mentioned reaction, ¹H-NMR, ¹³C-NMR, FT-IR, Mass Spectroscopy, and elemental analysis methods were employed to identify and explore the structure. Experimental and theoretical results were compared performing DFT calculations. The analysis of vibrational frequencies revealed that there was a good conformity between the experimental and theoretical results; so that, comparing the experimental and theoretical results, the value of R² was 0.999 for B3LYP, B3PW91, and mPW1PW91 theoretical methods. Furthermore, a good conformity was observed between the experimental and theoretical values of NMR spectroscopy. The results also indicated that by changing theoretical method the values of thermodynamic and HOMO-LUMO dependant parameters such as Chemical potential, Chemical hardness, Electrophilicity, and maximum amount of electronic charge transferred changed.

ACKNOWLEDGMENTS

The authors are indebted to Mr. Ehsan Fereyduni for their interest in this work and many helpful discussions. However this work was supported by Islamic Azad University Shahre-rey branch.

REFERENCES

1. Rajeeva. B, Srinivasulu. N, Shantakumar. S.M, *E-Journal of Chemistry*, **6**: 775 (2009).
2. Taghi-Ganji. K.M, Ghodsi. S.H, Alipour E, Amini. M, Hosseini. M, Shafiee. A, *Asian Journal of Chemistry*, **19**: 2521 (2007).
3. Bozdag-Dundar. O, Verspohl. E.J, Das-Evcimen. N, Kaup. R.M, Bauer. K, Sarikaya. M, Evranos. B, Ertan. R, *Bioorg Med Chem*, **16**: 6747 (2008).
4. Swarnkar. P.K, Kriplani. P, Gupta. G.N, Ojha K G, *E-Journal of Chemistry*, **4**: 14 (2007).
5. Ceriello. A, *Diab Met Res Rev*, **24**: 14 (2008).
6. Bozdag-Dundar. O, Ozgen. O, Mentese. A, Altanlar. N, Atli. O, Kendib. E, Eetana. R, *Bioorg Med Chem*, **15**: 6012 (2007).
7. Lee. H.W, Kim. B.Y, Ahn. J.B, Kang. S.W, Lee. J.H, Shin. J.S, Ahn. S.K, Lee. S.J, Yoon. S.S, *Eur J Med Chem*, **40**: 862 (2005).

8. Sahu. S.K, Banerjee M, Mishra. S.K, Mohanta. R.K, *Acta Pol Pharm Drug Res*, **64**: 121 (2007).
9. Eun. J.S, Kim. K.S, Kim. H.N, Park. S.A, Ma. T, Lee. K.A, Kim. D.K, Kim. H.K, Kim. I.S, Jung. Y.H, Zee. O.P, Yoo. D.J, Kwak. Y.G, *Arch Pharm Res*, **30**: 155 (2007).
10. Mori. M, Takagi. M, Noritake. C, Kagabu. S, *J Pestic Sci*, **33**: 357 (2008).
11. P.A. Nelson, G.D. Paulson, V. J. Feil, *Xenobiotica*, **17**: 829 (1987).
12. Verma. A, Saraf. S.K, *Eur J Med Chem*, **43**: 897 (2008).
13. Dwivedi. C, Gupta. T.K, Parmar. S.S, *J Med Chem*, **15**: 553 (1972).
14. I. Nabih , F. El-Hawary, H. Zoorob, *Journal of Pharmaceutical Sciences*, **8**: 1327 (1972).
15. Travis S. Young, Christopher T. Walsh, *PNAS*, **108**: 13053 (2011).
16. Tomas Tejero, Alessandro Dondoni, Isabel Rojo, Francisco L Merchán, Pedro Merino, *Tetrahedron*, **53**: 3301 (1997).
18. D. Davyt, G. Serra, *Mar. Drugs*, **8**: 2755 (2010).
19. E. Chamorro, M. Duque-Norea, P. Perez, *J. Mol. Struct. (THEOCHEM)* 896 (2009) 73.
20. R.G. Parr, L.V. Szentpaly, S. Liu, *J. Am. Chem. Soc.* 121 (1999) 1922.
21. Reza Solyemani, Y. M. Salehi, T. Yousofzad and Maryam Karimi-Chesmeh Ali, *Oreint. J. Chem.*, **28**(2): 627-638 (2012).
22. H. Aghabozorg, Sh. Moradi, E. Fereyduni, H. Khani, E. Yaaghubi, *Journal of Molecular Structure: THEOCHEM*, **915**: 58 (2009).
23. R. Dennington II, T. Keith, J. Millam, K. Eppinnett, W. Lee Hovell, R. Gilliland, GaussView, Version 3. 07, *Semichem, Inc.*, Shawnee Mission, KS, 2003.
24. M.J. Frisch, G.W. Trucks, H.B. Schlegel, G.E. Scuseria, M.A. Robb, J.R. Cheeseman, J.A. Montgomery, T. Vreven, K.N. Kudin, J.C. Burant, J.M. Millam, S.S. Iyengar, J. Tomasi, V. Barone, B. Mennucci, M. Cossi, G. Scalmani, N. Rega, G.A. Petersson, H. Nakatsuji, M. Hada, M. Ehara, K. Toyota, R. Fukuda, J. Hasegawa, M. Ishida, T. Nakajima, Y. Honda, O. Kitao, H. Nakai, M. Klene, X. Li, J.E. Knox, H.P. Hratchian, J.B. Cross, C. Adamo, J. Jaramillo, R. Gomperts, R.E. Stratmann, O. Yazyev, A.J. Austin, R. Cammi, C. Pomelli, J.W. Ochterski, P.Y. Ayala, K. Morokuma, G.A. Voth, P. Salvador, J.J. Dannenberg, V.G. Zakrzewski, S. Dapprich, A.D. Daniels, M.C. Strain, O. Farkas, D.K. Malick, A.D. Rabuck, K. Raghavachari, J.B. Foresman, J.V. Ortiz, Q. Cui, A.G. Baboul, S. Clifford, J. Cioslowski, B.B. Stefanov, G. Liu, A. Liashenko, P. Piskorz, I. Komaromi, R.L. Martin, D.J. Fox, T. Keith, M.A. Al-Laham, C.Y. Peng, A. Nanayakkara, M. Challacombe, P.M.W. Gill, B. Johnson, W. Chen, M.W. Wong, C. Gonzalez, J.A. Pople, Gaussian 03 Revision C.02, Gaussian Inc., Pittsburgh, PA, 2008.
25. B. Semire, O.A. Odunola, *Oriental journal of chemistry*, **25**: 841 (2009).
26. C.Y. Panicker, H.T. Varghese, A. Chandran, *Oriental journal of chemistry*, **27**: 1771 (2011).
27. C.Y. Panicker, H.T. Varghese, B. Harikumar, A. Chandran, *Oriental journal of chemistry*, **27**: 1705 (2011).
28. M. Taheri, R. Soleymani, B. Hosn, H. Rajabzadeh, M.R. Darvish, *Oriental Journal of Chemistry*, **28**: 387 (2012).
29. M.A. Boughdiri, O. Fliss, T. Boubaker, B. Tangour, *Oriental journal of chemistry*, **22**: 39052 (2006).
30. M.H Jamroz, *Vibrational Energy Distribution Analysis VEDA 4*, Warsaw, 2004.
31. K. Wolinski, J.F. Hinton, P. Pulay, *J. Am. Chem. Soc.* **112**: 8251-8260 (1990) .
32. K.R. Ambujakshan, H. Tresavarghese, S. Mathew, S. Ganguli, A. Kumar Nanda, C. Yohannan Panicker, *Oriental journal of chemistry*, **24**: 865 (2008).
33. L. Ushakumari, C.Y. Panicker, H. Tresavaraghese, Haseena, A.V. Vaidyan, N. Sudhakaran, K. Raju, *Oriental journal of chemistry*, **24**: 849 (2008).
34. H. Arslan, U. Flörke, N. K"ulc"u, G. Binzet, *Spectrochimica Acta Part A*, **68**: 1347 (2007).
35. S. Durmus, A. Atahan, M. Zengin, *Spectrochimica Acta Part A*, **84**: 1 (2011).
36. J. Coates, *Interpretation of Infrared Spectra, A Practical Approach*, John Wiley and Sons Ltd., *Chichester*, (2000).
37. X. Li, Z. Tang, X. Zhang, *Spectrochim. Acta A*, **74**: 168 (2009).
38. R. Saxena, L.D. Kuedpal, G.N. Mathur, *J. Polym. Sci. A: Polym. Chem*, **40**: 3559 (2002).

39. T. Shimanouchi, Y. Kakiuti, I. Gamo, *J. Chem. Phys.* **25**: 1245 (1956).
40. M.K. Rofouei, N. Sohrabi, M. Shamsipur, E. Fereyduni, S. Ayyappan, N. Sundaraganesan, *Spectrochimica Acta Part A*, **76**: 182 (2010).
41. M.K. Rofouei, E. Fereyduni, N. Sohrabi, M. Shamsipur, J.A. Gharamaleki, N. Sundaraganesan, *Spectrochimica Acta Part A*, **78**: 88 (2011).
42. V. Arjunan, C.V. Mythili, K. Mageswari, S. Mohanc, *Spectrochimica Acta Part A*, **79**: 245 (2011).
43. P. Politzer, D.G. Truhlar, *Chemical Application of Atomic and Molecular Electrostatic Potentials*, Plenum, New York, (1981).